SCIENTIFIC REPORTS

OPEN

SUBJECT AREAS:
FUEL CELLS
ELECTRONIC MATERIALS

Received
13 January 2014

Accepted
14 July 2014

Published
1 August 2014

Correspondence and requests for materials should be addressed to T.X. (twxu@ustc.edu.cn)

Oriented MOF-polymer Composite Nanofiber Membranes for High Proton Conductivity at High Temperature and Anhydrous Condition

Bin Wu[1], Jiefeng Pan[1], Liang Ge[1], Liang Wu[1], Huanting Wang[2] & Tongwen Xu[1]

[1]CAS Key Laboratory of Soft Matter Chemistry, Laboratory of Functional Membranes, School of Chemistry and Materials Science, University of Science and Technology of China, Hefei, Anhui, 230026(P.R. China), [2]Department of Chemical Engineering, Monash University, Clayton, Victoria 3800, Australia.

The novel oriented electrospun nanofiber membrane composed of MOFs and SPPESK has been synthesized for proton exchange membrane fuel cell operating at high temperature and anhydrous conditions. It is clear that the oriented nanofiber membrane displays the higher proton conductivity than that of the disordered nanofiber membrane or the membrane prepared by conventional solvent-casting method (without nanofibers). Nanofibers within the membranes are significantly oriented. The proton conductivity of the oriented nanofiber membrane can reach up to $(8.2 \pm 0.16) \times 10^{-2}$ S cm^{-1} at 160°C under anhydrous condition for the highly orientation of nanofibers. Moreover, the oxidative stability and resistance of methanol permeability of the nanofibers membrane are obviously improved with an increase in orientation of nanofibers. The observed methanol permeability of 0.707×10^{-7} cm^2 s^{-1} is about 6% of Nafion-115. Consequently, orientated nanofibers membrane is proved to be a promising material as the proton exchange membrane for potential application in direct methanol fuel cells.

Novel proton exchange membranes (PEMs) with high proton conductivity at temperature above 100°C can eliminate some serious problems facing PEM fuel cells including water and thermal management and CO poisoning[1–4]. The introduction of heterocycle (such as imidazole, triazole) into polymers has generated much interests in recent years with the hope that the imidazole-based membranes may solve the problems for the high temperature PEM fuel cells[5–8]. It is believed that heterocycle conducts protons through intermolecular proton shift and thus may be used to act as the proton carrier in proton-conducting materials above 100°C[5–8]. While the proton transfer has been surveyed in imidazole-based membranes, including polymers, oligomers or hybird material, the electrochemical stability of imidazole shows up inadequate for fuel cell performances because of the poisoning on the Pt electrode and high electronic density of imidazole ring[8–10]. 3-NH_2-1H-1,2,4-Triazole (Atz) has a similar molecular structure to that of imidazole and pyrazole, and therefore it may transmit protons by the similar mechanism as imidazole and pyrazole[11]. The pK_a(Acid dissociation constant)-values of Atz (pK_{a1} = 4.14, pK_{a2} = 9.97) are much lower than those of imidazole (pK_{a1} = 7.18, pK_{a2} = 14.52)[11–13], implying that Atz may have much higher acidity and lower electronic density, which tends to significantly influence proton conduction of Atz-based solid electrolytes. Similar to imidazole or pyrazole, Atz as a small molecule in a PEM may gradually leach out and ultimately lead to a continuous decrease in proton conductivity. The high proton conductive ability of triazole groups immobilized on a polymer chains may offer a new way to design PEMs with both high proton conductivity and long-term stability.

Metal-organic frameworks (MOFs), a new class of porous crystalline materials, act as an outstanding candidate in electrochemical field due to their high surface areas, controllable structures and potential electrochemical properties. Especially some MOFs exhibit proton conductivity or become proton conductive after introducing protonic charge carriers (water, acids, heterocycles) in their pores[14]. Our efforts have made on the design and synthesis of MOFs with good proton conductivity, aiming at overcoming the shortcomings of small molecule heterocycle. Since our initial attempts to synthesize MOFs by combining Atz with different metals did not yield highly crystalline structures, we decided to employ oxalic acid as co-ligand based on other prior success with the use of such a strategy in other systems[15]. The resulting porous Zn-aminotriazolato-oxalate compound, with a

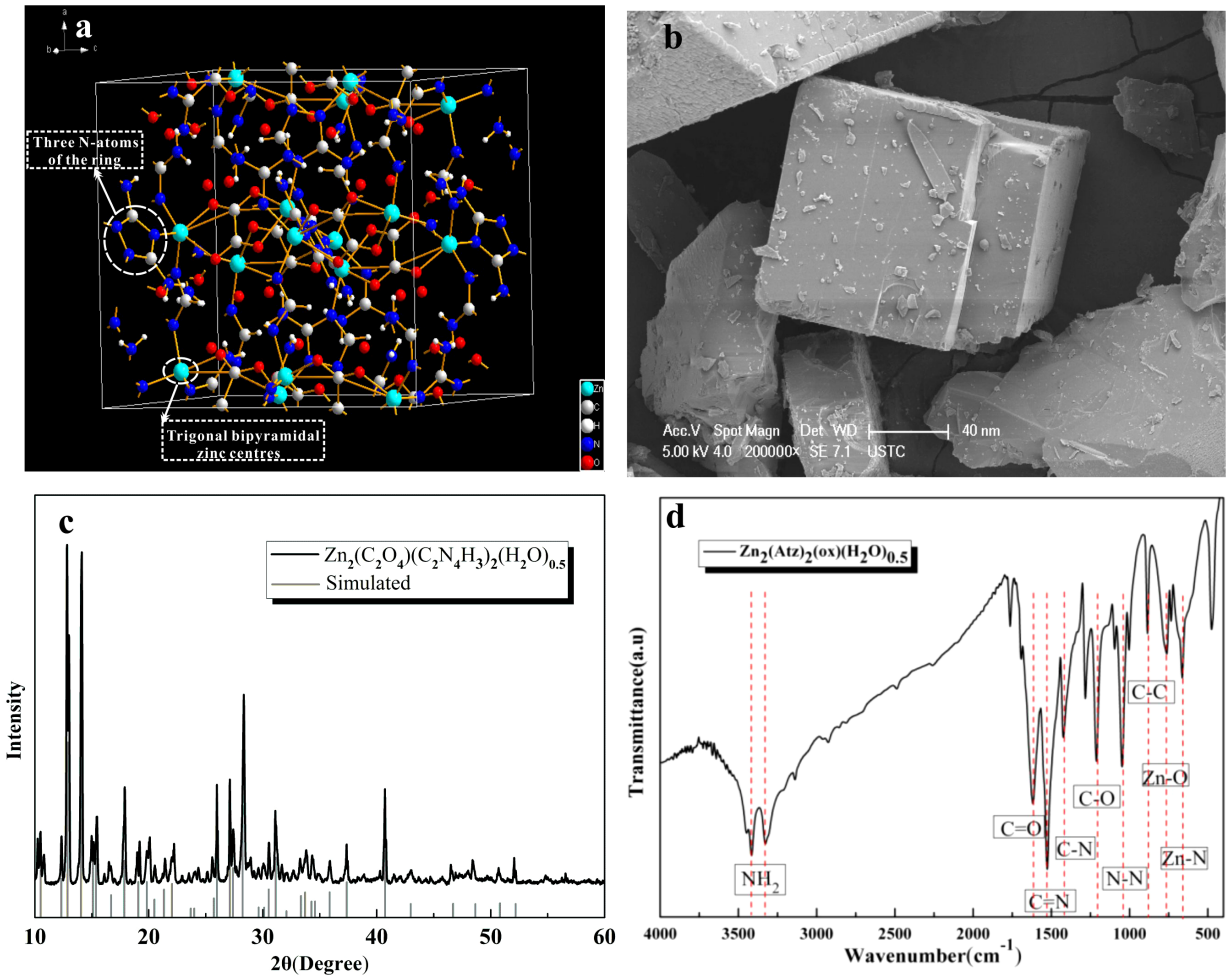

Figure 1 | (a) The three-dimensional structure formed by pillaring the above Zn-aminotriazolate layers by oxalate units. Color scheme: Zn-cyan; N-blue; O-red; C-grey; H-white. The cubic 6-connected network of ZCCH is indicated as white grids. b) SEM image of ZCCH microcrystal. c) Powder XRD for ZCCH (black) compared to that of the simulated (gray). d) FT-IR spectrum of ZCCH.

chemical formula $Zn_2(C_2O_4)(C_2N_4H_3)_2(H_2O)_{0.5}$(ZCCH), showed significant proton conductivity at high temperature and anhydrous condition but the bulk phase and grain boundary of ZCCH decreases the proton mobility, leading to a very low distance conductivity and discontinuous proton conductivity.

Recently, electrospun nanofibers have received considerable attention[16–20]. Electrospinning is capable of producing fibers with diameters in the nanometer range, and the electrospun nanofibers possess many unique properties such as large specific surface areas, superior mechanical properties, diversified composition, etc. However, there are only a few reports on the proton conductivity of electrospun nanofibrous mats[21–23]. If the electrospun membrane is prepared from oriented-aligned nanofibers with high proton conductivity, the protons may be rapidly transported through the nanofibers. We describe such oriented electrospun nanofibers membranes composed of sulfonated poly(phthalazinone ether sulfone ketone) (SPPESK) and ZCCH for use PEMs at high temperature and anhydrous condition. Our results show that these composite membranes exhibit dramatically enhanced proton conductivity and lower methanol permeability as compared with Nafion. This work offers a new strategy for the rational design and fabrication of high-temperature PEMs.

Results

ZCCH was synthesized via a solvothermal reaction[24]. Its schematic three-dimensional framework is shown in Figure 1a. SEM image of ZCCH crystal in Figure 1b exhibts a cube-shaped morphology. A typical powder XRD pattern of the ZCCH is shown in Figure 1c together with the simulated XRD pattern. The comparison between them demonstrates the formation of a pure phase ZCCH under the applied synthesis conditions. All results are consistent with those reported[24].

In the FT-IR spectrum (Figure 1d and Supplementary Figure S1) of ZCCH, the presence of 3-amino-1, 2, 4-triazole is indicated in the structure[25]. This observation is in agreement with previous FTIR studies on ZCCH, again confirming the structure of ZCCH[25]. The TGA curve of ZCCH is shown Figure S2 (Supplementary). When it was heated from 30 to 600°C, two weight-loss steps can be observed: first step occurs at 50–100°C is due to the solvent loss; second one starting from 300°C is resulted from the framework decomposition. Apparently, ZCCH crystal is thermally stable in the temperature range of 100°C to 300°C for the stable chelation of rigid linkers.

According to literature, sulfonation occurs only at the ortho-ether sites, the electron donating ether linkage of PPESK, because except for ether bond, all other groups attached to the aromatic rings contain more electron withdrawing functionality and will decrease the electrophilic reactivity of the polymers[26]. In this work, a mixture of 98% concentrated sulfuric acid and chlorosulfonic acid was selected as the sulfonating agent. The sulfonation procedure of PPESK is shown in Figure S3 (Supplementary). The comparative FTIR spectra of PPESK and SPPESK samples are shown in Figure S4 (Supplementary). All of these results obtained from the comparison of characteristic absorption bands between parent polymer and sulfonated

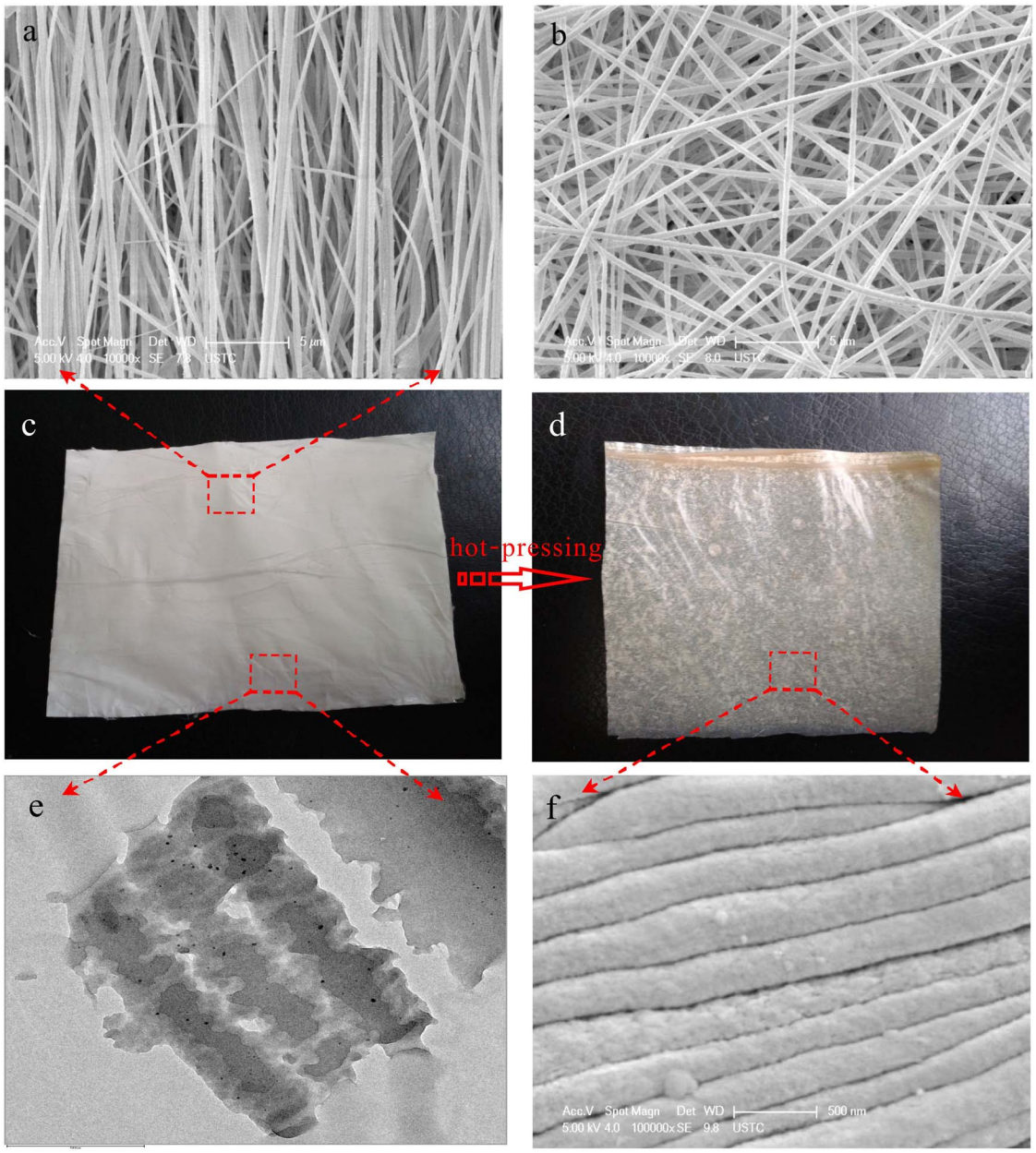

Figure 2 | Surface SEM of electrospun fiber mats at various surface velocities: (a) 5000 r/min, (b) 200 r/min. (c), (d) The optical photograph of oriented electrospun membrane before and after hot-pressing. (e). TEM of electrospun fiber mats. (f) Surface SEM of electrospun fiber mats after hot-pressing.

polymers confirmed the successful introduction of sulfonic acid groups into the polymer chains[27].

The synthetic procedure of PEMs solution is shown in Figure S5. There is Hinsberg reaction for connecting ZCCH with SPPESK. The ligands of ZCCH with amidogen of functionalities allow it to interact with the polymer material. In order to confirm the completion of the Hinsberg reaction, the IR spectrum and ^{1}HNMR of PPESK, SPPESK, chlorosulfonated SPPESK (PPESK-SO_2Cl) and electrospun membranes are shown in Figure S6, Figure S7 and FigureS8 (Supplementary), respectively. The asymmetric stretching appeared peak at 1374 cm^{-1} in the IR spectrum verifies the successful formation of $-SO_2Cl$. After reaction with ZCCH, the band totally disappeared and a new band at 1310 cm^{-1} appeared, corresponding to $-SO_2NH-$ group, which confirms the acid-amine bonding in electrospun nanofiber membranes[28]. The formation of chemical bonds between two-phase can avoid the phase separation and will improve the proton conductivity of the final PEMs.

The electrospinning process is a method of discharging a polymer solution in air from a nozzle under high voltage and producing a nanofiber by exploiting electrostatic repulsion of the polymer solution[29]. The schematic representation of the electrospun apparatus along with its side view is shown in Figure S9 (Supplementary), similar to that reported by Doshi and Reneker[29]. Figures 2a, b, c show the surface SEM and optical photograph of electrospun membranes prepared at two surface velocities of collector. It can be seen that the orientation of electrospun is achieved when increasing the surface velocity. It has been previously observed that the best alignment of the electrospun fibers in the membrane occurs when the linear velocity of the rotating cylinder surface matches that of evaporating jet depositions[30]. Thus, the optimum alignment surface velocity seems to be around the corresponding rotation speed of 5000 r/min in our case. Moreover, Fennessey and Farris reported that the maximum orientation was observed at the surface velocity[31], which was a comparable level to our value even though many processing parameters

Table 1 | Oxidative stabilities of membranes prepared using different fabrication methods

Membrane	Casting SPPESK-MOFs Membrane	Electrospun Disordered membrane	Electrospun Oriented membrane
oxidative stability (h)[a]	5.4	8.9	10.1

[a]Fenton stability was characterized after the membranes was completely dissolved in 3% H_2O_2 containing 2 ppm $FeSO_4$ at 80°C.

such as polymer type and solution concentration were different. To the best of our knowledge, this is the first report of the preparation of oriented nanofiber proton-conducting membrane based on ZCCH for the high temperature proton conduction. The pure electrospun membrane would adopt the hybrid inorganic-organic motif and form structural domains lined with SPPESK.

In the meantime, TEM of the oriented electrospun membrane is displayed in Figure 2e. It is shown that the ZCCH is of the cube structure when they are dispersed in the polymer matrix. The ZCCH not only are wrapped in PPESK-SO_2Cl, but also connected to the polymers. This good dispersion and contact are attributed to the formation of sulfimide. The optical photograph and surface SEM of the oriented electrospun membrane after hot-pressing are shown in Figures 2d and 2f. Other parameters affected by the collector rotation speed include the fiber diameter and its distribution (Supplementary Figure S10)[32,33]. The distribution of fiber diameter became much narrower with increasing surface velocity, and centered at about 200 nm in our study.

The structures of ZCCH, electrospun nanofiber membrane and electrospun nanofiber membrane after conductivity test of 160°C are examined by XRD (Supplementary Figure S11). All strong reflection peaks of the nanofiber membrane can be readily indexed to tetragonal ZCCH[24]. As manifested from the decreased peaks in XRD patterns, the ZCCH framework can still be kept after its interaction with SPPESK and conductivity test of 160°C. Nevertheless, the intensity of partial peaks is decreased or disappeared, because the ZCCH is wrapped in SPPESK. As for the TGA of electrospun membrane (Supplementary Figure S12), compared with the pure ZCCH, the decomposition temperature of the membrane is higher, because the frameworks are protected by the SPPESK wrapped on its surface.

The mechanical properties of electrospun membranes including the tensile strength (TS) and the elongation at the break (Eb) were measured at different temperatures. As shown in Figure S13 (Supplementary), even at high temperature, all membranes exhibited good mechanical properties, which are sufficient as proton exchange membrane. We also obtained the histograms of TS and Eb of membrane using different membrane fabrication techniques (Supplementary Figure S14). The mechanical strength of the nanofibers may be remarkably improved, because the polymers within the uniaxailly aligned nanofibers are strongly oriented in the axial direction of the nanofibers. In addition, as shown in Table 1, due to the orientation of fibers, the electrospun oriented membranes exhibited greater stability for Fenton's reaction than the casting membranes and electrospun disordered membranes.

Discussion

Proton conductivity measurement was performed on electrospun nanofiber membranes with disordered, oriented fibers and Nafion-115(Figure 3). The proton conductivities of the electrospun membranes were measured in transverse direction (i.e., parallel to the oriented nanofiber), although the proton transport current in a fuel cell was perpendicular to the membrane surface. The results show that Nafion-115 exhibits lower proton conductivity than the fiber membranes due to the decreased amount of water as a proton-conducting carrier. The oriented fiber membranes have higher conductivity than that of disordered fiber membrane at all temperatures. In addition, the proton conductivity of Nafion-115 increased firstly, and then decreased with the temperature due to the water loss; while those of the electrospun membranes increased with temperature due to the presence of triazole as the proton carrier instead of water. The conductivity of oriented nanofiber membrane at 160°C is found to be $(8.2 \pm 0.16) \times 10^{-2}$ S cm^{-1} (thickness is about 45 μm). The apparatus for this measurement is shown in Figure S15. This high-temperature proton conductivity is greater than that of any other MOFs-based materials to the best of our knowledge although some other polymers possess comparable proton conductivity under con-

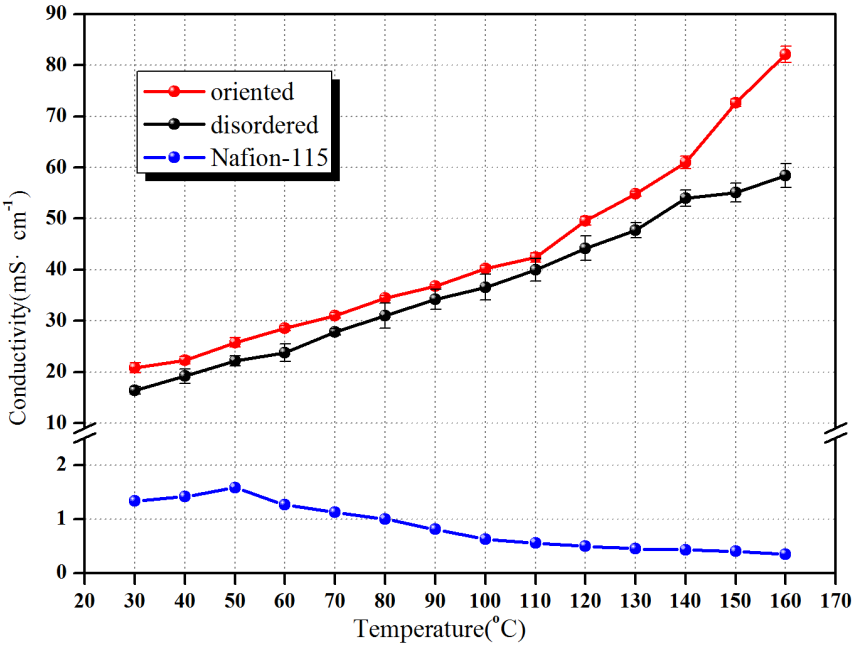

Figure 3 | Temperature-dependent proton conductivities of oriented, disordered nanofiber membranes and Nafion-115 under anhydrous condition.

ditions of using acidic and guest molecules[34]. For comparison, the conductivity of cast membrane was also measured and the data is shown in Figure S16. The results also show that the oriented fiber membranes have higher conductivity than that of casting membrane at all temperatures. Therefore, the addition of the ZCCH and the orientation of the nanofibers are responsible for the increase in proton conductivity.

For a direct methanol fuel cell, it also requires that the membranes have low methanol permeability. Here, the methanol permeability for oriented nanofiber membrane (in thickness of 49 μm) and Nafion-115(in thickness of 125 μm) has been tested under the same conditions, and the value is 0.707×10^{-7} cm^2 s^{-1} and 1.27×10^{-6} cm^2 s^{-1}, respectively. The value for oriented nanofiber membrane is about 6% of Nafion-115 (Supplementary Figure S17). The methanol permeability measurements in the electrospun composite membrane are carried out in the thickness direction. The obvious improvement can be attributed to the suppressed methanol diffusion induced by the oriented nanofibers structure and the introduction of ZCCH in the polymer matrix. In the meantime, the nitrogen from triazole and methanol can form hydrogen bonds, which could also reduce the methanol permeation. In other words, the frameworks of ZCCH help to entrap methanol, leading to highly selective proton conduction.

The polymers within the uniaxailly aligned nanofibers are strongly oriented in the axial direction of the nanofiber, and phase separation in the polymer having both hydrophobic and hydrophilic domains may be also facilitated. When the polymer having both hydrophobic and hydrophilic domains is electrospun, its hydrophobic and hydrophilic domains may segregate onto the outside as the air surface and the inside of the polymer solution, respectively. Consequently, the proton channel structure is formed within the nanofibers due to the network of the sulfamide and triazole ring, leading to a rapid transport of the proton within the proton transport sites (Figure 4)[35].

During the formation of nanofiber membranes, hydrophilic attractions between the triazole ring in ZCCH and sulfamide groups in SPPESK lead to the aggregation of ionic clusters into the interior[36]. These ionic clusters could contain protogenic groups from both sulfamide and Atz. The sulfonimide is a stronger acid compared to sulfonic acid, and can easily generate the protons at high temperature[37]. The protons migrates from polymers to ZCCH, transfer on the surface of ZCCH by hydrogen bonding and then to the next ZCCH via structural diffusion to form a complete conductive route, i.e. the protons transport follows Gratthuss mechanism (hopping mechnism). Consequently, the increased amount of interior protogenic groups form long-distance ionic pathways along the nanofibers that ensure effective proton transport through the entire membranes, as shown schematically in Figure 4a. To confirm these hypotheses, the phase separated structure in the nanofiber was observed using HRTEM (Figure 4b). The nanofiber was stained with Pb^+ ions. The dark areas represent hydrophilic domains and the light areas represent hydrophobic domains. HRTEM images in the axial directions reveal large amounts of hydrophilic groups within the nanofibers, which permit effective proton transport within the nanofibers.

We believe that the tautomerization and intramolecular proton transfer from Atz of ZCCH in the electrospun membrane may also play a vital role in the proton conducting process. Triazole-based systems have been reported to provide an advantage in proton transfer[38]. This is attributed to the presence of multiple tautomers for triazole, which would reduce the number of conformational changes required[38]. Atz can be viewed as a scaffold that can simultaneously provide proton conductive pathways in both the imidazole and the pyrazole modes (Supplementary Figure S18).

In summary, we have shown that the novel electrospun membranes containing uniaxially oriented SPPESK-ZCCH nanofibers can achieve high proton conductivity at high temperature and anhydrous condition, low methanol permeability and good chemical and thermal stabilities. At 160°C without humidification, a high proton conductivity of $(8.2 \pm 0.16) \times 10^{-2}$ S cm^{-1} is observed for the oriented nanofiber membrane, which is higher than the disorder nanofiber membrane or casting membrane. The methanol permeability for the oriented nanofiber membrane is 0.707×10^{-7} cm^2 s^{-1}, only 6% of Nafion-115. The membranes prepared in this study have great potential to improve the performance of PEM fuel cells at high temperatures. However, due to the current experimental limitations, the conductivity was measured in an in-plane way and the fuel cell performance was not conducted. For anisotropic membranes it would be necessary to show the through-plane conductivity as that what is really important for fuel cell operation. So how does the in-plane conductivity affect the fuel cell performance and what is the correlation between in-plane conductivity and through-plane one needs be further clarified.

Methods

Instrumentation. The samples were characterized by XRD with a Japan Rigaku Dmax X-ray diffractometer equipped with graphite monochromatized high-intensity Cu-Kα radiation (λ = 1.54178 Å). FT-IR spectra were recorded on KBr/ZCCH and all kinds of membrane about 25 ~ 30 μm in a Bruker model Vector 22 Fourier transform infrared spectrometer in transmission mode. The Spectrum are recorded on an AV III 400 NMR spectrometer (1H resonance at 400 MHz, Bruker) using DMSO-d6 (with tetramethylsilane as internal reference) as a solvent. TGA data were recorded on a TGA-50H analyzer from Shimadzu Instruments. Initially, the temperature was changed from 30°C to 600°C at a heating rate of 10°C min^{-1}. Measurements were

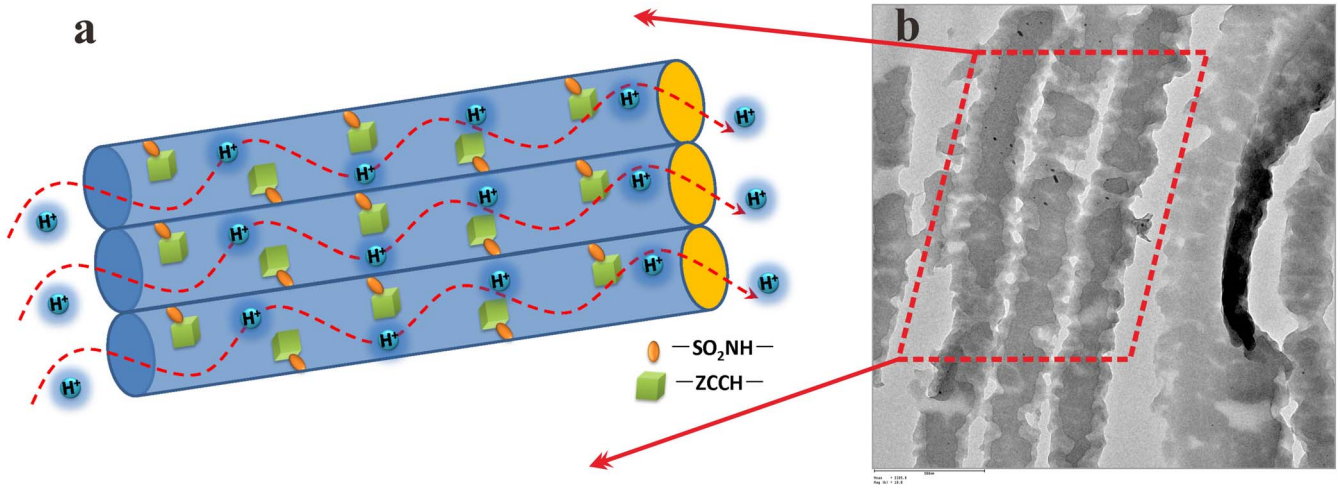

Figure 4 | (a) Schematic proton conductive process of oriented electrospun nanofiber. (b) HRTEM image of cross-sectional aligned nanofiber in axial direction.

carried out on a sample under a flow of N_2. The morphologies of membranes and ZCCH were investigated using SEM (XT30 ESEM-TMP PHILIP). Sample for HRTEM was prepared according to the following procedure: (1) the oriented electrospun membrane was stained in the saturated lead acetate solution for overnight. (2) Membranes was washed by distilled water, and then it was dried under vacuum at room temperature for 6 h. (3) Membrane was embedded in Spurr's epoxy resin in a block template and cured at ~60°C overnight. (4) The blocks were cut into slices about 50 ~ 90 nm thickness, using a Leica Ultracut ultramicrotome, and picked up on copper grids. Images were obtained using a Hitachi H7600 Transmission Electron Microscope with an accelerating voltage of 80 kV. Image J software was used to analyse the micrographs. The mechanical property test of the membrane was performed using a universal testing machine (INSTRON 5900 Testing System) at room temperature, 120°C and 160°C and crosshead speed of 10 mm min^{-1}.

Conductivity measurements. The four-probe AC impedance analyses were recorded using an Autolab® PGSTAT 302 (Eco Chemie, Netherlands) in galvanostatic mode (a.c. current amplitude = 0.1 mA, frequency range = 1 MHz to 50 Hz)[39]. Bode plots were used to determine the frequency region over which the magnitude of the impedance was constant; the ionic resistance was then obtained from the associated Nyquist plot. The measurements were carried out with the heating 1 ~ 2°C min^{-1} from ambient temperatures up to 160°C in air. The equipment was shows in Figure S15 (Supplementary). The proton conductivity (κ) was calculated according to the following equation:

$$\kappa = \frac{L}{RWd} \quad (1)$$

where R is the obtained membrane resistance, L is the distance between potential-sensing electrodes, and W and d are the width and thickness of the membrane, respectively.

Note that the conductivity of oriented and disordered membranes were measured for 3 times with error bars. However, Nafion-115 was only measured for 1 time due to the destroy after one cycle test and thus the error bar was not added.

Methanol permeability. The methanol permeability was measured using a self-made permeation-measuring cell with two compartments and mechanical stirring. Compartment A was filled with 100 cm^3, 5 mol L^{-1} methanol aqueous solution while compartment B with 100 cm^3 deionized water. The membrane was positioned between these two compartments with the effective diffusion area of 3.14 cm^2. During the experiment, the diffusion cell kept stirring slowly. The concentration of the methanol in compartment B was monitored by a refractive index detector (RI2000, Schambeck SFD Gmbh, Germany). The methanol permeability (P) was obtained using the following equation:

$$P = \left(\frac{C_t}{t}\right)_{slope} \times \frac{Vd}{AC_0} = \left(\frac{C_t}{U_t}\right)_{slope} \times \left(\frac{U_t}{t}\right)_{slope} \times \frac{Vd}{AC_0} \quad (2)$$

where $(C_t/U_t)_{slope}$ is predetermined as 1/17842 through standard curves, C_0 is the initial methanol concentration of the methanol solution, C_t is the methanol concentration in the deionized water-filled compartment at time t, V is the liquid volume in the deionized water-filled compartment, d is the thickness of the membrane, A is the effective permeation area and t is the time lag, i.e., the selected starting point for linear regressions.

MOFs Synthesis. Cube shaped colorless crystals of $Zn_2(C_2O_4)(C_2N_4H_3)_2(H_2O)_{0.5}$ were obtained from the reaction of a mixture containing 0.1 g of $2ZnCO_3 \cdot 3Zn(OH)_2$, 0.1 g of $H_2C_2O_4$ and 0.4 g of 3-amino-1,2,4-triazole, 3 mL of methanol and 0.5 mL of water at 180°C for 3 days (Yield: ~60% based on Zinc).

PPESK sulfonation. PPESK powder was dry for 24 h under 120°C in vacuum. It was dissolved in 50 ml of concentrated sulfuric acid of 98% under dry argon atmosphere. The mixture was heated to 90°C. The 10 ml of $ClSO_2OH$ (0.15 mol) dissolved in 30 ml of 98% concentrated H_2SO_4. The solution was added dropwise at the same temperature. The reaction mixture was vigorously stirred for 3 hr. The reaction mixture was dripped into the acetone under stirring, white sediment precipitation and filtering, then filtered content dissolved in DMAc and reprecipitation in the ether, twice the amount of precipitant for 20–500 (ml/g PPESK), reprecipitation product of filtering and acetone washing to neutral, in 120°C for 24 h under vacuum drying, SPPESK was obtained.

Preparation of oriented electrospun membranes. The SPPESK was dissolved in DMF and the chlorosulfonylation reaction of SPPESK was carried out under reflux of a DMF solution containing of thionyl chloride. The chlorosulfonylation of SPPESK (PPESK-SO_2Cl) was obtained by filtration, washed with water. The Hinsberg reaction was realized into PPESK-SO_2Cl of NMP solution blending with ZCCH and NaOH solution (0.1 mol L^{-1}). To achieved a homogeneous dispersion of the ZCCH particles, the solution was treated for 40 min in ultrasonic bath (KUDOS Ultrasonic 310, 53 Hz), afterwards it was stirred 3 d to prepare a uniform membrane solution.

The membranes were formed by the electrospun process. The typical electrospun parameters were as follows: The solutions were electrospun at 21 kV for 24–48 hours with a feed rate of 2.5 mm/min. Electrospun fiber mats were collected on the aluminum collector placed at a distance of 20 cm from the electrospun needle. The electric hot press was employed to compact the electrospun membrane with a pressure of 15 MPa for 15 min at 120°C after treatment for 15 min at DMF atmosphere of 30°C. The other membranes were formed by casting the membrane solution onto a flat glass surface. The casting equipment was placed on top of table an adjustable drying apparatus to assure horizontal alignment during the membrane formation and then evaporating the solvent at 60°C for 24 h. To prevent membrane contamination by dust particles during the evaporation of the solvent, evaporation pan was used to cover the glass. The membrane was removed from the glass surface by flushing with distillated water, when all the solvent was evaporated. The membrane was finally dried in a vacuum oven at 60°C. The thickness of the membranes was in the range of 50 ~ 60 μm. All the resulting membranes were treated with 1 M HCl aqueous solution for 24 h at room temperature. Finally, the membranes were washed with deionized water and dried in a vacuum oven at 60°C.

1. Paddison, S. J. Proton conduction mechanisms at low degrees of hydration in sulfonic acid-based polymer electrolyte membranes. *Annu. Rev. Mater. Res.* **33**, 289–319 (2003).
2. Wainright, J. S., Wang, J. T., Weng, D., Savinell, R. F. & Litt, M. H. ChemInform Abstract: Acid-Doped Polybenzimidazoles: A New Polymer Electrolyte. *J. Electrochem. Soc.* **142**,121–123 (1995).
3. Casciola, M. & Alberti, G. Layered metal (IV) phosphonates, a large class of inorgano-organic proton conductors. *Solid State Ion* **97**, 177–186 (1997).
4. Haile, S. M., Boysen, D. A., Chisholm, C. R. I. & Merle, R. B. Solid acids as fuel cell electrolytes. *Nature* **410**, 910–913 (2001).
5. Kreuer, K. D., Fuchs, A., Ise, M. & Spaeth, M. Imidazole and pyrazole-based proton conducting polymers and liquids. *Electrochim. Acta* **43**, 1281–1288 (1998).
6. Munch, W., Kreuer, K. D., Silvestri, W., Maier, J. & Seifert, G. The diffusion mechanism of an excess proton in imidazole molecule chains: first results of an ab initio molecular dynamics study. *Solid State Ion* **145**, 437–443 (2001).
7. Schuster, M. F. H., Meyer, W. H., Schuster, M. K. & Kreuer, D. Toward a new type of anhydrous organic proton conductor based on immobilized imidazole. *Chem.Mater.* **16**, 329–337 (2004).
8. Noda, A. *et al.* M. Bronsted acid-base ionic liquids as proton-conducting nonaqueous electrolytes. *J. Phys. Chem. B.* **107**, 4024–4033 (2003).
9. Yang, C., Costamagna, P., Srinivasan, S., Benziger, J. & Bocarsly, A. B. Approaches and technical challenges to high temperature operation of proton exchange membrane fuel cells. *J. Power Sources* **103**, 1–9 (2001).
10. Deng, W., Molinero, V. & Goddard, W. A. Fluorinated imidazoles as proton carriers for water-free fuel cell membranes. *J. Am. Chem. Soc.* **126**, 15644–15645 (2004).
11. Catalan, J., Abbound, J. L. & Elguero, M. J. Basicity and acidity of azoles. *Adv. Heterocycl. Chem.* **41**, 187–274 (1987).
12. Gagliano, R. A., Knowlton, R. C. & Byers, L. D. Methylimidazole-Catalyzed Ester Hydrolysis: Nonlinear Kinetics. *J. Org. Chem.* **54**, 5247–5250 (1989).
13. Walba, H. R. & Isensee, W. Spectrophotometric Study of the Acid Strength of Imidazole. *J. Org. Chem.* **21**, 702–704 (1956).
14. Yoon, M., Suh, K. S. & Natarajan, K. K. Proton Conduction in Metal-Organic Frameworks and Related Modularly Built Porous Solids. *Angew. Chem. Int. Ed.* **52**, 2688–2700 (2013).
15. Rao, C. N. R., Natarajan, S. & Vaidhyanathan, R. Metal carboxylates with open architectures. *Angew. Chem. Int. Ed.* **43**, 1466–1496 (2004).
16. Drew, C. *et al.* Metal oxide-coated polymer nanofibers. *Nano Lett.* **3**, 143–147 (2003).
17. Huang, J. X. & Kaner, R. B. Flash welding of conducting polymer nanofibres. *Nat. Mater.* **3**, 783–786 (2004).
18. Dzenis, Y. Spinning continuous fibers for nanotechnology. *Science* **305**, 1917–1919 (2004).
19. Patel, A. C., Li, S., Yuan, J. M. & Wei, Y. In situ encapsulation of horseradish peroxidase in electrospun porous silica fibers for potential biosensor applications. *Nano Lett.* **6**, 1042–1046 (2006).
20. Formo, E., Lee, E., Campbell, D. & Xia, Y. Functionalization of electrospun TiO_2 nanofibers with Pt nanoparticles and nanowires for catalytic applications. *Nano Lett.* **8**, 668–672 (2008).
21. Na, H. *et al.* Fabrication of sulfonated poly(ether ether ketone ketone) membranes with high proton conductivity. *J. Membr. Sci.* **281**, 1–6 (2006).
22. Elabd, Y. A., Snyder, J. D. & Chen, H. Electrospinning and solution properties of Nafion and poly(acrylic acid). *Macromolecules* **41**,128–135 (2008).
23. Wycisk, R., Pintauro, P. N., Mather, P. T., Choi, J. & Lee, K. M. Nanofiber network ion-exchange membranes. *Macromolecules* **41**, 4569–4572 (2008).
24. Ramanathan, V. S., Simon, I., Karl, W. D. & George, K. H. S. An amine-functionalized metal organic framework for preferential CO_2 adsorption at low pressures. *Chem. Commun.* **35**, 5230–5232 (2009).
25. Kandiah, M. *et al.* Synthesis and Stability of Tagged UiO-66 Zr-MOFs. *Chem. Mater.* **22**, 6632–6640 (2010).
26. Ramanathan, V. *et al.* Direct Observation and Quantification of CO_2 Binding within an amine-functionalized nanoporous solid. *Science* **330**, 650–653 (2010).
27. Takuya, T. & Hiroyoshi, K. Aligned electrospun nanofiber composite membranes for fuel cell electrolytes. *Nano Lett.* **10**, 1324–1328 (2010).
28. Sata, T., Izuo, R. & Takata, K. Layeformation on a Cation-exchange membrane by acid amide bonding, and transport-properties of the resulting membrane. *J. Membr. Sci.* **45**, 197–208 (1989).

29. Doshi, J. & Reneker, D. H. Electrospinning process and applications of electrospun fibers. *J. Electrostat.* **35**, 151–160 (1995).
30. Matthews, A., Wnek, G. E., Simpson, D. G. & Bowlin, G. L. Electrospinning of collagen nanofibers. *Biomacromolecules* **3**, 232–238 (2002).
31. Fennessey, S. & Farris, F. J. Fabrication of aligned and molecularly oriented electrospun polyacrylonitrile nanofibers and the mechanical behavior of their twisted yams. *Polymer* **45**, 4217–4225 (2004).
32. Deitzel, J. M., Kleinmeyer, J., Harris, J., Beck, D. & Tan, N. C. The effect of processing variables on the morphology of electrospun nanofibers and textiles. *Polymer* **42**, 261–272 (2001).
33. Demir, M. M., Yilgor, M. I., Yilgor, E. & Erman, B. Electrospinning of polyurethane fibers. *Polymer* **43**, 3303–3309 (2002).
34. Umeyama, D., Horike, S., Inukai, M., Hijikata, Y. & Kitagawa, S. Confinement of Mobile Histamine in Coordination Nanochannels for Fast Proton Transfer. *Angew. Chem. Int. Ed.* **50**, 11706–11709 (2011).
35. Savard, O., Peckham, T. J., Yang, Y. & Holdcroft, S. Structure-property relationships for a series of polyimide copolymers with sulfonated pendant groups. *Polymer* **49**, 4949–4959 (2008).
36. Kim, T., Choi, Y. W., Kim, C. S., Yang, T. H. & Kim, M. N. Sulfonated poly(arylene ether sulfone) membrane containing sulfated zirconia for high-temperature operation of PEMFCs. *J. Mater. Chem.* **21**, 7612–7621 (2011).
37. Jannasch, P. Recent developments in high-temperature proton conducting polymer electrolyte membranes. *Curr. Opin. Colloid. In.* **8**, 96–102(2003).
38. Zhou, Z., Li, S. W., Zhang, Y. L., Liu, M. L. & Li, W. Promotion of proton conduction in polymer electrolyte membranes by 1H-1,2,3-triazole. *J. Am. Chem. Soc.* **127**, 10824–10825 (2005).
39. Sone, Y. & Ekdunge, P. D. Simonsson Proton conductivity of Nafion 117 as measured by a four-electrode AC impedance method. *J. Electrochem. Soc.* **143**, 1254–1259 (1996).

Acknowledgments

The authors thank for financial supports from the National Basic Research Program (No.2012CB932800), the National Natural Science Foundation of China (Nos. 21128004, 51273185, 21025626) and National High Technology Research and Development Program 863 (2012AA03A608).

Author contributions

B.W. and J.P. designed the project; B.W. and J.P. carried out the experiment with help from L.G. and L.W.; B.W., H.W. and T.X. wrote the manuscript. All authors discussed the results and commented on the manuscript.

Additional information

Supplementary information accompanies this paper at http://www.nature.com/scientificreports

Competing financial interests: The authors declare no competing financial interests.

How to cite this article: Wu, B. *et al.* Oriented MOF-polymer Composite Nanofiber Membranes for High Proton Conductivity at High Temperature and Anhydrous Condition. *Sci. Rep.* **4**, 4334; DOI:10.1038/srep04334 (2014).